British Journal of Pharmacology-Special issue
246 words in abstract
4488 words excluding abstract, methods, acknowledgments, refs & legends
8 Figures and 2 Tables plus supplementary material
55 Refs

In vitro and *in vivo* characterisation of the bifunctional MOP/DOP ligand UFP-505.

N. Dietis[1], H. Niwa[1], R. Tose[1], J McDonald[1], V. Ruggieri[2], M. Filaferro[3], G. Vitale[4], L. Micheli[5], C. Ghelardini[5], S Salvadori[6], G. Calo[6], R. Guerrini[7], D.J. Rowbotham[8] and D.G. Lambert[1].

[1] Department of Cardiovascular Sciences, University of Leicester, Division of Anaesthesia, Critical Care and Pain Management, Leicester Royal Infirmary, Leicester, UK.

[2] Department of Oncology Haematology and Respiratory Diseases, University of Modena & Reggio Emilia, Modena, Italy.

[3] Dept. Biomedical, Metabolical and Neuro-Sciences, University of Modena and Reggio Emilia, Modena, Italy;

[4] Section of Pharmacology, Department of Life Sciences, University of Modena and Reggio Emilia, Modena, Italy

[5] Department of Preclinical and Clinical Pharmacology, University of Florence, Florence, Italy.

[6] Department of Experimental and Clinical Medicine, Section of Pharmacology, University of Ferrara, Ferrara, Italy.

[7] Department of Pharmaceutical Sciences, University of Ferrara, Ferrara, Italy.

[8] Department of Health Sciences, University of Leicester, Division of Anaesthesia, Critical Care and Pain Management, Leicester Royal Infirmary, Leicester, UK.

Address correspondence and reprint requests to Prof D.G. Lambert at the above address. Tel: +44 (0)116 258 5694 E.mail DGL3@le.ac.uk

Present address for ND, Medical School, University of Cyprus, 1 University Avenue, Aglantzia 2109, Nicosia, Cyprus. For HN and RT, Department of Anesthesiology, University of Hirosaki, Hirosaki, Japan. HN and RT contributed equally to this work.

This article has been accepted for publication and undergone full peer review but has not been through the copyediting, typesetting, pagination and proofreading process which may lead to differences between this version and the Version of Record. Please cite this article as doi: 10.1111/bph.14199

Funding and COI statement:

Work on bifunctional opioids in the University of Leicester is funded by HOPE Foundation for Cancer Research (www.hfcr.org). RG. SS and GC are members of a University spin-out company, *University of Ferrara Peptides* (UFPeptides) that is involved in the development of opioid ligands. Other listed authors are collaborators with UFPeptides. UFP-505 is not subject to patent and may be made available on request to RG/SS

Short running title: Pharmacology of bifunctional opioid UFP-505

Author Contributions:

DGL, GC, RG, SS, DJR and ND involved in the planning and design of the study. ND collected or co-ordinated the collection of all data. HN, RT and JMcD were involved in collection of in vitro data in Leicester. VR, MF, GV and ND collected *in vivo* data in Modena, Italy. LM and CG collected *in vivo* data in Florence, Italy. All authors were involved in interpretation of the data and approved the final draft of the manuscript.

Keywords: MOP receptor, DOP receptor, opioid, bifunctional, beta-arrestin, internalization, antinociception, tolerance, morphine.

Acknowledgements: This work has been supported by HOPE Against Cancer (www.hfcr.org). ND was the recipient of the British Pharmacological Society Schachter Award (www.bps.ac.uk). We would like to thank Dr David Lodwick and Sonja Khemiri for their help with the novel cell line production and Prof T Costa for his constructive advice on receptor internalization.

ABSTRACT

Background and purpose: Targeting more than one opioid receptor type simultaneously may have analgesic advantages in reduced side effect profile. We have evaluated the mixed MOP (μ, mu) agonist/DOP (δ, delta) antagonist UFP-505 *in vitro* and *in vivo*.

Experimental approach: We measured receptor density and function in single MOP, DOP and MOP/DOP double expression systems. GTPγ^{35}S binding, cAMP formation and arrestin recruitment were measured. Antinociceptive activity was measured *in vivo* using tail withdrawal and paw pressure tests following acute and chronic treatment. In some experiments we have harvested tissue to measure receptor.

Key Results: UFP-505 bound to MOP and DOP; at MOP this binding resulted in full agonist activity and at DOP there was low efficacy partial agonism. At MOP but not DOP UFP-505 treatment led to arrestin recruitment. Unlike morphine, UFP-505 treatment internalized MOP and there was evidence for DOP internalization. Similar data were obtained in a MOP/DOP double expression system. In rats, acute UFP-505 or morphine treatment was antinociceptive following i.t. administration. In tissues harvested from these experiments there was a reduction in MOP and DOP receptor density for UFP-505 but not morphine (in agreement with in vitro data). Both Morphine and UFP-505 induced significant tolerance.

Conclusions and Implications: In this study we have shown that UFP-505 behaves as a full agonist at the MOP receptor with variable activity at DOP. This bifunctional compound produces antinociception in rats via i.t. administration. In this paradigm dual targeting provides no advantages in terms of tolerance liability.

Non-standard abbreviations: WHO, World Health Organisation; CHO, Chinese Hamster Ovary Cells; DAMGO, [D-Ala^2, NMe-Phe^4, Gly-ol^5]-enkephalin; DPDPE, [D-Pen^2,D-Pen^5]-enkephalin; UFP- 505, H-Dmt-Tic-Gly-NH-Bzl; DPN, Diprenorphine; EM1, Endomorphin1; GTPγ^{35}S, guanosine 5′-[γ-^{35}S-thio]triphosphate; GAPDH, Glyceraldehyde 3-phosphate dehydrogenase; MOP, mu opioid receptor; DOP, delta opioid receptor; KOP, kappa opioid receptor; N/OFQ, Nociceptin/Orphanin FQ; NOP, N/OFQ receptor.

INTRODUCTION

Opioids have been the main treatment option for pain for centuries but their use is associated with a number of troublesome side effects, including respiratory depression, constipation, immune suppression, physical dependence and tolerance (Sehgal et al., 2013). Analgesic tolerance is a long term process, which is distinct to the rapid process of desensitization that arises from chronic administration of opioids (Dang & Christie 2012). When analgesic tolerance occurs, the patient requires increasingly higher doses of the drug in order to reach sufficient analgesia. Since these higher doses result in increased side effects, including tolerance itself, it is easy to appreciate that tolerance drives an inevitable vicious clinical circle of increasing doses and increased side effects, which is the end result of chronic opioid use (Dietis et al., 2009). Clinically, an increase in opioid analgesia can be achieved by switching opioid or adding an adjuvant and the WHO analgesic ladder describes this from a practical standpoint. However, a short-term increase in analgesia does not attenuate the development of tolerance and therefore a reduction in the degree of analgesia achieved is inevitable. Therefore, reducing the propensity for tolerance in novel opioids is an efficient strategy for providing quality analgesia without detrimental dose-escalation.

Opioid receptors are members of a large family: μ (mu, MOP), δ (delta, DOP), κ (kappa, KOP) and the 'opioid-like' Nociceptin/Orphanin FQ (N/OFQ) receptor; NOP (Dietis et al., 2011; Lambert 2008). Almost all clinically available (and pharmaceutical developed) opioid analgesics target mainly the MOP receptor, although there is current evidence for constitutive interactions among receptor subtypes (dimerization) that might change the way we think about the drug-target relationship of opioids (Gupta et al., 2006). With relevance to our study, the most functionally-important interaction of opioid receptors occurs between the MOP and DOP receptors (Law et al., 2005). Gomes and colleagues provided evidence that MOP-DOP dimers possess functional and ligand binding synergy (Gomes et al, 2000), whereas George and colleagues showed a distinct binding profile of opioid ligands at MOP-DOP dimers (George et al, 2000). More interestingly however, a number of earlier studies in rodents have shown that when the DOP receptor is blocked by an antagonist (Abdelhamid et al., 1991; Hepburn et al., 1997) or its gene is knocked out (Zhu et al., 1999) or knocked down (Kest et al., 1996), or the gene for the endogenous DOP receptor agonist enkephalin is knocked out (Nitsche et al., 2002), then tolerance to morphine is reduced.

From a drug development perspective, it is preferable to use a single molecule to simultaneously target the MOP and DOP receptors rather than co-administering two drugs, both from a pharmacokinetic point of view and reduced drug interactions. For this purpose, two chemical types of opioids can be considered; *bifunctional opioids* (e.g. opioids that have two distinct binding properties) and *bivalent opioids* (e.g. opioids that possess two distinct pharmacophores in their structure) (Dietis et al., 2009). Although these two types of 'dual' opioids have been well described in the literature during the last decade, their differentiation in terms of advantages in chemical design or molecular efficacy is not yet clear.

Our group has used the bifunctional opioid UFP-505 (H-Dmt-Tic-Gly-NH-Bzl) as a prototype MOP receptor agonist and DOP receptor antagonist (Balboni et al., 2010; Dietis et al., 2012) and hypothesized that this opioid ligand will produce antinociceptive actions *in vivo* with reduced analgesic tolerance liability. Here, we present our data from relevant *in vivo* assays on the tolerance, as well as new data on the ligand's effects on opioid receptor density and trafficking from *in vitro* (at recombinant MOP, DOP and MOP/DOP double expression receptor systems) and *ex vivo* (rat tissues) assays.

METHODS

Additional information for the materials used can be found in the online supplement.

Cell culture

CHO cells stably expressing a single type of human opioid receptor (hMOP and hDOP) and cells with high expression of hDOP receptors ($CHO_{hDOP/high}$) were grown as described previously (Dietis et al., 2012). Stock cultures were supplemented with 200 $\mu g.ml^{-1}$ geneticin (G418), for CHO_{hMOP}, CHO_{hDOP} and $CHO_{hDOP/high}$ cells, and with additional 200 $\mu g.ml^{-1}$ hygromycin B for the novel $CHO_{hMOP/hDOP}$ cell line. Cell cultures were kept at 37 °C in 5% CO_2/humidified air and subcultured as required using trypsin/EDTA. Cells were used for experimentation as they approached confluence and were selection agent free.

Novel cell line stably expressing hMOP and hDOP

A novel CHO cell line stably expressing the human MOP and DOP receptors ($CHO_{hMOP/hDOP}$) was produced by transfecting geneticin-resistant CHO_{hMOP} cells with human DOP receptor cDNA in a hygromycin B-selectable vector (pcDNA3.1Hygro(+)/OPRD1; S&T Missouri

University, USA) and selected with 800 μg.ml^{-1}.hygromycin B and 500 μg.ml^{-1} geneticin (GIBCO, UK). Initially, the transfection of hDOP in CHO_{hMOP} cells produced a polyclonal mixture which was further sub-cloned producing a final number of 30 $CHO_{hMOP/hDOP}$ clones. To narrow the selection for the appropriate monoclonal cell batch, all clones were screened by qRT-PCR and their MOP and DOP receptor mRNA expression levels were determined. The top 3 clones that showed the highest transfection efficiency were used in radioligand binding assays to determine receptor protein expression. One clone was selected for use and binding data are described in results. Cell culturing of $CHO_{hMOP/hDOP}$ cells was as described above with double selection pressure.

Saturation-binding assay to determine receptor density

Membrane protein from CHO cells (70–100 μg; prepared as described in the supplement) was incubated in 0.5 ml volume of 50 mM Tris, 0.5% BSA, with a variety of peptidase inhibitors (amastatin, bestatin, captopril, phosphoramidon) at 10 μM and various concentrations of radioligand ^{3}H-DPN for 1 h at room temperature. Tritiated DAMGO (^{3}H-DAMGO) and tritiated naltrindole (^{3}H-NT) was used for labelling MOP and DOP receptors respectively in saturation binding assays as appropriate. In some experiments (as noted in results) full saturation analysis was performed and in others a saturating radioligand concentration was used. Non-specific binding (NSB) was defined in the presence of 10 μM naloxone. Reactions were terminated and bound/free radioactivity was separated by vacuum filtration through polyethylenimine (0.5%)-soaked Whatman GF/B filters, using a Brandel harvester. Bound radioactivity was determined after 8 h extraction in ScintisafeGel (Wallac, Loughborough, UK) using liquid scintillation spectroscopy.

Displacement binding assay to determine ligand selectivity and binding affinity

Membrane protein (70–100 μg) was incubated as in saturation assays, but containing ~1 nM ^{3}H-DPN and varying concentrations (1 pM - 10 μM) of a range of displacer ligands. NSB was defined in the presence of 10μM naloxone. Assay incubation time, reaction termination, and bound radioactivity were the same as in the saturation assay.

GTPγ^{35}S assay to determine ligand functional activity

Membrane protein (70–100 μg) was incubated in 0.5 ml volume of 50 mM Tris, 0.2 mM EGTA, 1 mM $MgCl_2$–$6H_2O$, 100 mM NaCl, pH 7.4 supplemented with 0.1% BSA, 0.15 mM

bacitracin, GDP (33 μM) and ~150 pM GTPγ^{35}S with gentle shaking for 1 h at 30ºC. NSB was determined in the presence of non-radiolabelled 10 μM GTPγS. Reactions were terminated by vacuum filtration through dry Whatman GF/B filters, using a Brandel harvester. Bound radioactivity was determined as in the saturation assays. Endomorphin-1, [D-Pen^2,D-Pen^5]-enkephalin (DPDPE) or UFP- 505 (H-Dmt-Tic-Gly-NH-Bzl) were included where appropriate at various concentrations and combinations as described in the Results section.

Inhibition of forskolin-stimulated cAMP formation

CHO whole cell suspensions were incubated in 300 μl Krebs'/HEPES buffer (143 mM NaCl, 4.7 mM KCl, 2.6 mM $CaCl_2$, 1.2 mM $MgSO_4$, 1.2 mM KH_2PO_2, 12 mM glucose and 10 mM HEPES, pH to 7.4) containing 0.5% BSA, 1 mM IBMX, 1 μM forskolin and 10 μM of endomorphin-1, DPDPE and UFP-505. Reactions were incubated for 15 min at 37 °C, with gentle shaking, terminated by addition of 20 μl 10M HCl, neutralised by addition of 20 μl 10M NaOH and buffered to pH 7.4 by addition of 200 μl 1M Tris–HCl. Cellular debris was cleared by centrifugation and resulting supernatant assayed for cAMP formation, against cAMP standards, in a competitive binding assay with [^{3}H] cAMP using a binding protein extracted from bovine adrenal glands as described previously (Kitayama et al., 2007). Bound and free radioactivity were separated by the addition of 250 μl of charcoal mixture (250mg charcoal, 100 mg BSA per 25 ml solution, 50 mM Tris-HCl and 4mM EDTA buffer at pH 7.4). Each tube was allowed to stand for 1min before centrifugation at 12000 g in a Sarstedt microfuge at RT. The supernatant (200 μl) was taken and mixed with 1ml of Optiphase Hi-Safe scintillation liquid and radioactivity was counted using liquid scintillation spectroscopy.

Receptor internalization and receptor desensitization assays

For the internalization study, cells (grown in large T175 flasks) were incubated with appropriate concentration of a given ligand in 20 ml of fresh culture medium for an appropriate time according to the experiment and as described in results. Adherent cells were then washed three times at 4 °C with harvest buffer (containing 0.9% Saline, 0.02% EDTA, 10mM HEPES, pH of 7.4) to remove any receptor-bound ligand, before harvesting. Membranes were prepared as previously described (Dietis et al., 2012), washing three times with buffer prior to three centrifugations at 1600 g and three centrifugations at 14000 g, with subsequent removal of supernatant and resuspension of the pellet, in order to ensure that all desensitising ligand is washed off. Then, a saturation binding assay was performed as described above. For receptor internalization, CHO_{hMOP} cells where treated with 10 μM of morphine, EM1 or fentanyl and

CHO_{hDOP} with 10 μM DPDPE, as reference compounds with the maximum concentration used in these experiments, as well as with various concentrations of UFP-505 (1 nM-10 μM) for CHO_{hMOP} or 10 μM for CHO_{hDOP}. For the desensitization studies, cells were incubated for 1 hour (chosen as most appropriate for tolerance-related desensitisation; based on Williams et al., 2013) with an appropriate ligand at various concentrations (1 pM - 10 μM) and membranes were prepared as in the internalization study. A GTPγ^{35}S assay was then performed as described above.

Arrestin assay

The PathHunter® eXpress Chinese hamster ovary (CHO)–K1 pre-validated cell lines were used (DiscoveRx, Birmingham, UK), expressing human MOP or DOP receptors and β-arrestin-2, supplied in an optimized cell culture medium. The assay measures binding of β-arrestin with the receptor of interest upon activation by an agonist. The assay was performed according to manufacturer's instructions. Briefly, cells were thawed and plated in OCC medium in 96-well luminescence plates and allowed to recover for 48 hours at 37 °C. Agonists were added in each well respectively and incubated for 90 minutes at 37 °C. Detection reagents were added and incubated with the cells for 60 minutes at room temperature. Chemiluminescence was measured using a standard 96 well plate luminometer.

Animal handling

Healthy male Wistar rats (strain code 003, albino, 200-250 g/rat) were used in the tail-flick antinociception assay (TF) and healthy male Sprague-Dawley rats (Harlan, Varese, Italy, 280-300 g/rat) were used in the paw-pressure (PP) and rotarod assays. All animals were obtained from Charles Rivers Laboratories. Before any surgical or experimental procedures, all animals were housed in groups of two-three under standard controlled conditions (22±1 °C, 12 h light/dark cycle) with food and water *ad libitum* for at least 5 days. Animal weight and evident behavioural changes were monitored prior, during and after each experiment. After surgery and during experiments, all animals were housed as one per cage. All animals were used at least one week after their arrival in the lab. Ethical guidelines for investigation of experimental pain in conscious animals were followed; all experiments were conducted in line with the European Directive (EEC No. 86/609) and the Italian D.L. 27/01/1992, No.116 and the University of

Florence or Modena Animal Subjects Review Board and were in accordance with the ARRIVE guidelines (Kilkenny et al., 2010).

Intrathecal surgery

We initially used an intrathecal catheterization protocol for animals used in the acute tail-flick test, but it was not possible to retain the catheters on these animals for long-term exposure (data not shown), therefore we elected to use an alternative catheterisation strategy for the rest of the tests used (rotarod and paw-pressure). Below, we describe both protocols used. For the tail-flick test, animals were anaesthetized by intraperitoneal (i.p.) ketamine and xylazine (115 +2 mg/kg ; Farmaceutici Gellini, Aprilia, Italy and Bayer, Milan, Italy) and a modification of the Strokson method of intrathecal (i.t.) catheterization was applied (Storkson et al., 1996) at the lumbar region of the spinal cord (between the L5 and L6; figure 1S in the supplement). After surgery, the correct catheter positioning was assessed by lidocaine administration (15 μl, 20 mg/ml, *i.t.*) followed by saline (10 μl, *i.t.*) and subsequent loss of motor control of the rear limbs within 15 sec lasting for 20-30 mins. One animal that did not pass this lidocaine-test was excluded from the study.

For the animals used in the rotarod and paw-pressure assays, these were anesthetized with 2% isoflurane and the intrathecal catheter was surgically implanted according to the Yaksh and Rudy method (Yaksh and Rudy, 1976). Rats were shaved on the back of the neck and placed in the stereotaxic frame with the head securely held between ear bars. The skin over the nap of the neck was cleaned with ethyl alcohol and incised for 1 cm. The muscle on either side of the external occipital crest was detached and retracted to expose about 3-4 mm^2 of the atlanto-occipital membrane. The membrane was incised by a needle, which led to the escape of cerebrospinal fluid. The caudal edge of the cut was lifted and about 7.0 cm of 28 g polyurethane catheter (0.36 mm outer diameter; 0.18 mm inner diameter; Alzet, USA) was gently inserted into the intrathecal space in the midline, dorsal to the spinal cord until the lumbar enlargement. The exit end of the catheter was connected to 4.0 cm polyurethane (0.84 mm outer diameter; 0.36 mm inner diameter) and was taken out through the skin, flushed with saline solution, sealed and securely fixed on the back of the head with a silk suture. The incision site in the skin was sutured with polyamide suture and animals were allowed to recover for 24 h before the study began. The evaluation of potential motor dysfunctions induced by the surgery was investigated using a rota-rod test. Any animals displaying motor disabilities (approximately 10%) were excluded from the paw-pressure behavioural measurements.

Tail-flick test

Animals were submitted to the tail-flick test (15 sec cut-off time) prior to acute *i.t.* treatment of varying drug concentrations in order to determine their nociceptive threshold (basal latency; BL), and after *i.t.* administration of drugs at times T = 15, 30, 60, 90 and 120 mins to determine treatment latency (TL). The control-group animals were treated with sterile saline (20 µl) whereas the treatment group animals was treated with 10µl (i.t.) of UFP-505 followed by administration of sterile saline (10µl i.t.). Morphine was also used as a reference compound in a separate animal group, in a protocol similar to the treatment group.

Rotarod test

The rotarod apparatus (Ugo Basile, Varese, Italy) was consisted of a base platform and a rotating rod with a diameter of 6 cm and a non-slippery surface. The rod, 36 cm in length, was placed at a height of 25 cm from the base and was divided into 4 equal sections by 5 disks. Thus, up to 4 rats were tested simultaneously on the apparatus, with a rod-rotating speed of 10 r.p.m. The integrity of motor coordination was assessed on the basis of the number of falls from the rod during 60 seconds in acute protocol and 120 seconds during the repeated one. The test was stopped after a maximum of 6 falls.

Paw-pressure test

The mechanical nociceptive threshold in the rat was determined with a paw-pressure test (PP, Ugo Basile, Varese, Italy), according to the method described by Leighton et al. (Leighton et al., 1988). A constantly increasing mechanical pressure was applied to the animal's paw, until occurrence of vocalization or withdrawal reflex, while rats were lightly restrained. Vocalization or withdrawal reflex threshold levels were expressed in grams of the applied pressure. Animals with basal threshold below 40 g or above 75 g were excluded prior to treatment. Measurements were performed after acute i.t. injection of 0.3-30 nmol UFP-505 (10 µl). Antinociception was measured at 15, 30, 45 and 60 min after administration with a PP test. Chronic experiments (8 days) involved i.t. daily of 10 nmol UFP-505 or 3 nmol morphine (in 10 µl) and antinociception in paw-pressure (along with motor coordination using a rotarod; as described above) was evaluated every day at 30 min after administration. The cut-off threshold for treated animals in this assay was 150 g. Experiments of paw-pressure and motor coordination were performed blind from each other.

Tissue removal

Animals used in the TF test were killed by decapitation immediately after the end of each experiment and their spinal cord tissue and cerebral cortex were isolated while on ice. Tissues were stored at -80 °C and used later for membrane preparation as described above. Part of the tissues scheduled for later PCR analysis were first treated with RNA*later*® solution (AM7020, Applied Biosystems, USA), then stored at -20 °C for two days and finally stored at -80 °C for three days.

Data analysis

All data are presented as mean ± SEM from (n) experiments, as shown in the figure/table legends. Concentration–response curves were analysed by non-linear regression using GraphPad Prism V5.0 software (San Diego, CA, USA). In saturation-binding assays, the receptor density (B_{max}) and radioligand equilibrium dissociation constant (pK_d) were obtained from saturation-binding isotherms and semi-log transformations of specific binding data. In displacement binding assays, 50% displacement of specific binding was corrected for the competing mass of radiolabel and the pK_i values were obtained from displacement curves and values were determined using non-linear regression, corrected using the Cheng-Prusoff equation Prusoff (Cheng & Prusoff 1973) ($\log\{EC_{50}/(1+[L]/K_d)\}$), where EC_{50} is the effective concentration of the ligand that displaces 50% of the radioligand, [L] the concentration of the radioligand used, and K_d the dissociation constant of the radioligand. pEC_{50} and E_{max} values in functional experiments were obtained from the sigmoidal curve with a variable slope. All statistical analysis was performed using GraphPad Prism V5.0 software (San Diego, CA, USA). Some data were analyzed using the "Origin 9" software. Students t-test and analysis of variance (ANOVA) with post-hoc testing (Bonferroni) as required were used as described in the table and figure legends (significance set at $p<0.05$).

Nomenclature of Targets and Ligands

Key protein targets and ligands in this article are hyperlinked to corresponding entries in http://www.guidetopharmacology.org, the common portal for data from the IUPHAR/BPS Guide to PHARMACOLOGY (Harding et al., 2018), and are permanently archived in the Concise Guide to PHARMACOLOGY 2017/18 (Alexander et al., 2017).

RESULTS

In vitro characterization of UFP-505

In part of the present study we have used DOP-expressing cells with receptor density (figure 1A-left ~1.8pmol mg protein^{-1}), ~1.8 higher than the reported value in (Dietis et al., 2012). In membranes prepared from these high-DOP expressing cells, we found significant but low partial-agonist activity for UFP-505 in a GTPγ^{35}S assay (α 0.28 relative to DPDPE), as shown in figure 1A-right, indicating a partial- DOP agonism at very high (non-physiological) receptor density. The potency of UFP-505 (pEC_{50}; 8.54±0.28) was significantly higher than that of DPDPE (7.68±0.20; $p<0.05$) in membranes from these cells.

Downstream from G-protein activation forskolin stimulated cAMP formation in CHO_{hMOP} cells was inhibited by both 1 μM EM1 and 10 μM UFP-505, as shown in figure 1B. There was no significant difference between the inhibition of cAMP formation caused by EM1 and UFP-505, indicating that UFP-505 behaves as a full agonist in this downstream amplified assay. In CHO_{hDOP} cells, 10 μM DPDPE inhibited forskolin-stimulated cAMP formation as expected for a DOP full agonist (figure 1B). However, the addition of 10μM UFP-505 resulted in a small, but significant, inhibition of forskolin-stimulated cAMP (α0.23 relative to DPDPE), again suggesting that UFP-505 behaves as a low efficacy DOP partial-agonist in this highly amplified assay. This is an important point in discussing the behaviour of the ligand *in vivo* at target 'sites' with higher expression.

In vitro receptor internalization

Next we examined the effects of UFP-505 on opioid receptor turnover. Pre-treatment of CHO_{hMOP} cells with 10 μM UFP-505 produced a significant loss of surface MOP receptors (62%) compared to the non-treated cells (figure 2A). In the same assay, pre-treatment with 10μM EM1 and fentanyl produced significant MOP receptor internalization (~50% and ~25% respectively), whereas morphine was ineffective. To determine whether time of ligand pre-treatment had an effect on the reduction of MOP receptor density, binding assays with saturating radioligand concentrations were performed after pre-treatment of CHO_{hMOP} cells with 10 μM UFP-505 for 1 hour and 24 hours. Pre-treatment of UFP-505 (Control B_{max} 457±86) for 24 hours induced internalization of MOP receptors (B_{max} 166±15) in a similar manner to pre-treatment for 1 hour (B_{max} 108 ± 23); this difference was not significant (by One-Way ANOVA analysis with Bonferroni correction).

The decrease in MOP receptor density induced by UFP-505 was concentration-dependent, as shown in figure 2B. UFP-505 induced a significant MOP receptor internalization at 10 μM and 1 μM compared to the control (untreated), with a pEC_{50} of 6.62. This is similar with the pEC_{50} produced from GTPγ^{35}S binding (6.37) but lower than the pK_i of UFP-505 binding (7.79) as shown in previously published data (Dietis et al., 2012).

Interestingly, in CHO_{hDOP} cells (figure 2C; B_{max}~1000fmol/mg protein) where UFP-505 behaves as a low efficacy partial agonist, 10 μM of UFP-505 induced extensive DOP receptor internalization (~86%) in a similar manner to the DOP full agonist DPDPE at 10μM (~80%). The unexpectedly-extensive DOP receptor internalization by UFP-505, based on its weak intrinsic activity, raised an initial concern that the reduction seen in this assay could be an artefact, possibly due to an incomplete wash-off of the desensitising challenge. In order to exclude this possibility, full ^{3}H-DPN saturation curves were produced from CHO_{hMOP} and CHO_{hDOP} cells pre-treated with 10 μM UFP-505 after wash off and the pK_d was calculated (figure 3). Representative saturation curves are shown here, from a series of five independent experiments performed after pre-treatment with 10 μM fentanyl in CHO_{hMOP} cells (figure 3B) and 10 μM UFP-505 (figure 3C). The pK_d of the curves produced were not different from the control (figure 3G), confirming that the reduced radioligand binding shown in the internalization assays and interpreted as a reduction in the B_{max} is attributed solely to the internalization of the receptors and not to the presence of residual UFP-505 in the assay. Similarly, representative saturation curves from CHO_{hDOP} cells (from n=5) after pre-treatment with 10 μM DPDPE (figure E) and 10 μM UFP-505 (figure F) are also shown here and the resulting pK_d of the curves from all pre-treatment groups did not differ from the control. Arrestin recruitment is a facet of the internalisation process so we used the PathHunter® to compare arrestin recruitment with internalisation.

Arrestin recruitment

In CHO_{hMOP} cells, UFP-505 induced a concentration-dependent recruitment of β-arrestin to the MOP receptor with a pEC_{50} of 6.91 (figure 4A), which was not significantly different to the pEC_{50} of morphine (6.75). However, at 10 μM, morphine showed significantly lower E_{max} than UFP-505, EM1 and fentanyl, whereas EM1 and fentanyl showed significantly higher E_{max} than UFP-505. For the DOP receptor, although DPDPE produced a concentration-dependent recruitment of β-arrestin upon receptor activation, UFP-505 did not (figure 4B). We do not

know receptor density of the cells used in this assay as they were provided ready-to-go by the assay manufacturer.

In vitro characterization of the double-expression system

All of our *in vitro* work to date has been with a single expression system so in order to mimic the *in vivo* situation in a simple system we produced a CHO MOP/DOP double expression system. Our selected monoclonal $CHO_{hMOP/hDOP}$ batch has B_{max} of 672±34 and 159±32 $fmol.mg^{-1}$ (mean ± SEM) for the MOP and DOP receptors respectively, using tritiated naltrindole (^{3}H-Nt) and DAMGO (^{3}H-DAMGO) as a DOP-selective and MOP-selective radioligands in saturation binding assays. This gave a MOP:DOP ratio of 4:1. In addition, full saturation curves with the non-selective ligand ^{3}H-DPN confirmed the overall expression levels of both types of opioid receptors to be 851±45 $fmol.mg^{-1}$ as shown in figure 5A (the numerical sum of individual MOP; 672 and DOP; 159, was 831 $fmol.mg^{-1}$, similar to that determined by ^{3}H-DPN).

Displacement binding assays showed an 'overall' DPN pK_d of 9.51 ± 0.19 for the double-expression $CHO_{hMOP/hDOP}$ cells, similarly to the pK_d produced for CHO_{hMOP} and CHO_{hDOP} cells (Dietis et al., 2012). The binding of ^{3}H-DPN in $CHO_{hMOP/hDOP}$ membranes was displaced in a concentration-dependent manner by UFP-505 and three reference ligands; endomorphin-1 (EM1), naltrindole and morphine (figure 5B). The 'overall' binding affinity (pK_i) of UFP-505 in $CHO_{hMOP/hDOP}$ membranes was 7.70±0.16 (n=5), whereas the binding affinities for the respective reference ligands were to be 7.53±0.10 (endomorphin-1), 7.87±0.07 (naltrindole) and 7.75±0.11 (morphine) respectively.

The capacity of UFP-505 to induce receptor internalization in the mixed MOP and DOP receptor population was then studied. UFP-505 induced ~62% opioid receptor internalization (MOP and DOP), significantly higher than morphine which did not induce significant internalization compared to control (figure 5C). Pre-treatment of DPDPE and EM1 produced ~27% and ~43% internalization respectively.

In the GTPγ^{35}S assay, pre-treatment of $CHO_{hMOP/hDOP}$ cells with EM1 or UFP-505 produced a significant reduction in the efficacy (E_{max}) of both ligands, without change in potency (pEC_{50}) (figure 6). The next step from a simple double expression system was to examine behaviour *in vivo* in standard antinociceptive assays acutely and in a chronic paradigm to assess tolerance.

In vivo characterization of UFP-505

TF test: UFP-505 produced a time- and dose-dependent antinociceptive response (figure 7). Treatment with 10 and 50 but not 1 and 3 nmol UFP-505 produced a significant response. Furthermore, animals treated with 50nmol UFP-505 reached and retained the cut-off time from the first sampling point (15 mins) throughout the study to 120 mins (figure 7A). Intrathecal morphine 10 nmol produced a similar antinociceptive profile to UFP-505 10 nmol, which was not significantly different from 15 minutes until 90 minutes after injection. However, morphine antinociception was significantly reduced at 120 minutes after injection. An analysis of UFP-505 dose-response curves for latency at 120 min after administration and area under curve (AUC; sec/min) from figure 7A, are shown in figure 7B. The pED_{50} values calculated for each curve were found to be very similar (8.20±0.05 and 8.19±0.18 respectively; equivalent ED_{50} values 6.27 and 6.38 nmol respectively).

Rota-rod test: In both acute tests using the animals from the paw-pressure animal group there were no significant effects on performance at doses up to and including 10 nmols. At 30 nmols UFP-505 there was marked impairment of locomotor activity of the posterior paws; at the 15min time point the cut-off of 6 falls was reached (Table 1).

Paw pressure test: Acute administration of UFP-505 produced an antinociceptive response that peaked at 15-30 mins. Compared to pre-test values there was a significant response in 30 and 10nmol does at 15 and 30 mins (figure 8A). Based on the mechanical threshold at 15 mins a crude ED_{50} of ~9 nmol can be estimated; similar to that obtained in the TF assay. In Figure 8B the effects of daily administration of 3nmol morphine and 10 nmol UFP-505 are shown; based on previous data (Micheli et al, 2015) this dose of morphine is equi-effective to 10 nmol UFP-505 in an acute setting. By day 6-7 animals were tolerant to both morphine and UFP-505. There were no differences in the time course for induction of tolerance between the two ligands.

Ex vivo study of neuronal tissue from treated animals in the TF study

We had the opportunity to extract and harvest the neuronal tissue from the treated rats in order to assess the receptor turnover *in vivo* and to compare the produced data with our *in vitro* data. Membrane from lysates of isolated rat neuronal tissue (cortex and spinal cord) of acutely treated animals (UFP-505, morphine and saline) were used for labelling the MOP and DOP receptors with tritiated DAMGO (^{3}H-DAMGO) and tritiated naltrindole (^{3}H-Nt), in a series of independent binding assays with saturating concentrations of radioligand. Processing of these

membranes was based in the same procedure as in membranes from cell lysates described in methodology. Receptor density values (B_{max}) were calculated and density changes were expressed in % difference from saline treated animals, as shown in Table 2. Administration of morphine did not induce any changes in receptor density in the frontal cortex for both MOP and DOP receptors. In contrast, treatment with UFP-505 induced a loss of cell-surface MOP and DOP receptors in this tissue, compared to morphine-treated and untreated membranes. Additionally, for the spinal cord samples, the effect of UFP-505 and morphine on cell-surface receptor numbers was similar (internalization MOP: 44.7%, DOP: 43.1%). A reduction in density of both receptors was observed in the UFP-505 treated samples compared to the expression of the respective receptors in the morphine and untreated samples, Table 1. The ineffectiveness of morphine to internalize the MOP receptor agrees with other studies (Whistler & Von Zastrow, 1998; Zhang et al., 1998; Bohn et al., 2004) and with the rest of internalization data presented later here.

Additionally, the cortex and spinal cord tissue from treated and non-treated animals were pooled in two discrete groups and processed as two batches to determine opioid receptor mRNA expression by RT-qPCR (expressed as ΔC_t - cycle threshold difference values compared to GAPDH; shown in supplement, table 1S). In acutely morphine-treated animals variable changes in opioid receptor mRNA levels were observed for all opioid receptors across all tissues examined. One interesting change that stood out is that acute i.t. morphine and UFP-505 treated animals showed upregulation of the MOP receptor mRNA in the spinal cord, but only morphine-treated animals showed simultaneous upregulation of the DOP receptor. The data with morphine align with findings from other studies showing that exposure to morphine leads to an increase in the surface expression of DOP in cultured cortical neurons and in neurons in the dorsal horn of the spinal cord *in vivo* (Morinville et al., 2003; Cahill et al., 2001), although these findings were based on a 48 hour exposure to morphine. Furthermore, in the frontal cortex, only the KOP receptor mRNA levels were shown to upregulate in morphine-treated animals. In the rest of the cortex, only the DOP receptor mRNA levels were shown to significantly down regulate in both treatment groups. Finally, in the same tissues, NOP receptor mRNA levels were down regulated in both treatment groups.

DISCUSSION

Bifunctional opioids have long been studied in opioid pharmacology, either for exploring the relationship between different receptor types or aiming to produce opioid ligands with reduced adverse effects (Dietis et al., 2009; Schiller 2010). In this study we show that UFP-505 behaves as a full agonist at the MOP receptor and displays a variable expression dependent efficacy at the DOP receptor. This bifunctional compound produces antinociception in rats via i.t. administration.

Partial agonism depends on expression levels

At intermediate DOP expression and in an unamplified system, UFP-505 behaves as a competitive DOP antagonist (Dietis et al., 2012) and at very high expression levels in an amplified system, UFP-505 can display a partial-agonist activity. This behaviour agrees with our previous observations that partial agonist behaviour is largely depended on receptor expression levels (McDonald et al., 2003). Indeed, in CHO_{hDOP} cells we were able to unmask low efficacy in a GTPγ^{35}S assay (0.28 relative to DPDPE; unamplified, with DOP levels at ~2 pmol/mg protein) and in cAMP assay (amplified, with DOP levels at ~1 pmol/mg protein). No activity was shown by UFP-505 in the commercial arrestin assay (unamplified, with DOP receptor expression levels unknown) whereas full agonist activity was shown for the loss of cell surface receptors (amplified, with DOP levels at ~1 pmol/mg protein).

Reduced radioligand binding translates to true loss of cell surface receptors

The accuracy of receptor expression determined by radioligand labelling is sensitive to 'sticky' ligands that remain bound to receptors, since they may reduce radioligand binding that can be misinterpreted as reduced receptor density. In our standard experimental protocol we use extensive washing when using natural peptide ligands and radiolabelling (Hashimoto et al., 2002). However, we also constructed a full saturation curve to [^{3}H]DPN in both MOP and DOP receptor cell lines, in order to provide evidence of effective wash-off, with the resulting K_d of the radioligand being unaffected, indicating there was no residual desensitising challenge present at the receptor. We therefore conclude that the reduction in radioligand binding represents a true loss of cell surface receptors. In addition, we show loss of cell surface receptors in well washed membranes from tissues extracted from whole animals.

Arrestin recruitment and receptor internalization

Control of post-receptor signalling lies in a co-ordinated interplay between receptor activation and loss of cell surface receptors by endocytosis (internalization). The recruitment of β-arrestin-2 (βArr) plays a central role to the internalization of opioid receptors and other GPCRs (Zuo 2005). Early studies showed that morphine fails to internalize the membrane MOP receptors (Keith et al., 1996) and stimulation of MOP receptor endocytosis by enhanced βArr can counteract the development of morphine tolerance (Koch et al., 2005). Nevertheless, the involvement of βArr in morphine tolerance is more complicated than a straight forward linear effect, since the reduction of cellular βArr may also attenuate morphine tolerance (Yang et al., 2011; Wang et al., 2016). In our assay, activation of MOP receptors caused the recruitment of βArr with a rank order of E_{max} EM1>Fentanyl>UFP-505>Morphine. UFP-505 was able to recruit the βArr significantly more than morphine. Despite UFP-505 being a low efficacy partial agonist at the DOP receptor and able to induce internalisation, the ligand did not show any significant βArr recruitment. We do not know the level of DOP receptor expression in this commercial assay, so it is possible that the lack of a partial agonism response by UFP-505 in the DOP-expressing cells of this assay could be due to the low receptor expression in this system, unmasked only at higher levels. On the other hand, there are mechanisms of receptor internalization that are βArr-independent (Van Koppen et al., 2004; Bradburry et al., 2009) and whether these mechanisms are part of UFP-505 activity is unknown. In addition, the ability of a ligand to resensitize the MOP receptor and promote recycling is also an important factor for its tolerance profile (Dang & Christie, 2012), an aspect for UFP-505 that needs to be clarified. In essence, UFP-505 is shown to be a ligand unlike morphine in its ability to induce MOP receptor internalization and therefore seems to have the potential to produce reduced analgesic tolerance compared to morphine.

In vitro studies with a double expression system

We aimed to simulate the *in vivo* situation, where MOP and DOP receptors are co-expressed, by producing a stable recombinant $CHO_{hMOP/DOP}$ double expression system. In this system, morphine failed to internalize both receptors and UFP-505 was more effective than EM1 in internalizing the MOP receptor, data that are consistent with the single MOP expression system. There was a reduced ability of DPDPE to internalize the DOP receptor and whilst it is tempting to suggest that this may potentially result from the dimer, it could be simply a result of the relatively lower density of DOP receptors compared to MOP in this cell line.

MOP and DOP receptors have been shown to co-localise *in vivo* (Wang et al., 2005) and their constitutive dimerization plays a functional role in disease and ligand pharmacology (Yekkirala et al., 2012; Stockton & Devi 2012). Double-expression recombinant systems have been previously used and showed that the potency of opioids may differentiate compared to single-opioid receptor expression cell lines (Yekkirala et al., 2012; Yekkirala et al., 2010). Moreover, the response of these opioids in the MOP/DOP co-expression system has been shown to be reversed with naltrindole, suggesting a functional interaction between the two receptors. This is in agreement with (Waldhoer et al., 2005) who showed that heterodimer activation (by 6-guanidinonaltrindole) was tissue specific and only occurred at the level of the spinal cord. Collectively, these data suggest that DOP receptor blockade can reduce the efficacy of morphine when the MOP receptor is co-expressed, which agrees with the premise of our study that since DOP receptor antagonism reduces morphine tolerance it may explain why UFP-505 has reduced tolerance liability. In the longer term, if DOP receptor antagonism reduces MOP receptor signalling, then it is possible that this could have a 'protective effect' on MOP receptors, reducing their ability to desensitise. More importantly, there is evidence to suggest that receptor dimer numbers do change in chronic pain (Costantino et al., 2012), supporting the claims of a vital physiological role of these receptor dimers in disease. Certainly UFP-505 is able to produce internalisation and does not behave like morphine in this respect. In our double expression system the potency of UFP-505 is greater by 5-fold than in the single MOP expression system, suggesting that our bifunctional ligand is interacting with a functional MOP-DOP heterodimer. Clearly further experimentation with tagged opioid receptors and UFP-505 are required.

In vivo experiments

Acute i.t. injection of UFP-505 produced a robust antinociceptive response in the tail-flick assay with potency (ED_{50}) of ~7 nmoles; 10 nmoles of UFP-505 was found as equi-antinociceptive to 10nmoles of morphine. More importantly, our data show that UFP-505 produced prolonged antinociception that persisted more than 120mins after acute administration, compared to a faster-declining morphine antinociception. Similar data were obtained in the paw-pressure test (using a different catheterisation strategy) with and ED_{50} for UFP-505 of ~9 nmols. These data confirm for the first time the presumption of a strong antinociceptive dose-dependent effect of UFP-505 as a MOP receptor ligand with agonist activity. Morphine tolerance has been consistently reported to manifest in rats after 3 days with i.t. treatment (Grandos-Soto et al., 2000) or 5 days with s.c (Goodchild et al., 2009) and i.p

(Chen et al., 2008). We confirmed these findings for morphine with our long-term testing using the paw-pressure test. Bifunctional ligands with MOP agonist and DOP antagonist profile have been shown to have reduced tolerance profile (Mosberg et al., 2014) and therefore we expected that UFP-505 would show a similar profile in our long-term tests of paw-withdrawal, given its pharmacological profile *in vitro* and its shown analgesic efficacy *in vivo*. However, to our surprise, UFP-505 produced a tolerance profile that was not significantly different from that of morphine in our model. Although we have no data that will offer a mechanistic explanation of UFP-505's tolerance profile, there are two factors that could explain this discrepancy. The first is the antinociception model used. Different pain models (e.g. tail-flick, hot-plate, paw-pressure, warm water tail-withdrawal, capsaicin administration, acetic acid writhing) utilize different types of nociceptive stimuli (e.g. electrical, thermal, mechanical, chemical) that require the involvement of a mixed variety of neuronal processes (Bars et al., 2001). Given the complex molecular changes that occur during long-term exposure of opioids and the stimuli differences between antinociceptive models, it is possible that the development of nociceptive tolerance is model-sensitive. Another potential factor for UFP-505 tolerance profile is the dose and method of administration used. Some recent studies have suggested a dose dependence of opioid tolerance induction (Pawar et al., 2007; Madia et al., 2009) which increases the difficulty of efficiently comparing data from studies that use different opioid doses and routes of administration. A more simple explanation is possible based on the observed residual agonist activity at DOP; this may become important in producing tolerance. Studies with a *pure* DOP antagonist are warranted.

Nevertheless, the profile of tolerance liability in opioids that possess a bi- or multi-functional activity profile is not new. A characteristic example of such a ligand is buprenorphine, a well-known and fully-characterised complex opioid that has been studied for more than 40 years (Lutfy and Cowan, 2004). Although buprenorphine is a MOP partial agonist, a DOP and a KOP antagonist (Huang et al., 2001) its tolerance profile has been somewhat similar to morphine (Paronis and Bergman, 2011). Nevertheless, the pharmacokinetic profile and a lack of a ceiling effect in the clinical setting is seen as an advantage (Louis 2006; Khanna and Pillarisetti 2015).

The main aim of the study was to fully characterize a promising bifunctional ligand (based on earlier data) and provide insights on the potential relationship between in vitro and in vivo activity. Full characterisation of a bifunctional opioid with multiple in vitro/ex vivo/in vivo assays is important but not often performed. Our data presents a continuum from basic

pharmacology to antinociception. Specifically this study of UFP-505 (*in vitro* and *in vivo)* offers invaluable information on the pharmacological properties that bifunctional opioids may present. Unfortunately, the lack of antinociceptive efficacy of UFP-505 in non-systemic routes of administration (e.g. subcutaneous route; see supplementary Figure-1) may preclude further development as a potential future clinical opioid; the insights and offered from studying UFP-505 are of utility in the drive to produce newer opioid molecules with increased antinociceptive efficacy and reduced tolerance.

REFERENCES

Abdelhamid EE, Sultana M, Portoghese PS, Takemori AE (1991). Selective blockage of delta opioid receptors prevents the development of morphine tolerance and dependence in mice. J Pharmacol Exp Ther 258(1): 299-303.

Alexander SPH, Christopoulos A, Davenport AP, Kelly E, Marrion NV, Peters JA, Faccenda E, Harding SD, Pawson AJ, Sharman JL, Southan C, Davies JA; CGTP Collaborators. (2017) The Concise Guide to PHARMACOLOGY 2017/18: G protein-coupled receptors. Br J Pharmacol. 174 Suppl 1: S17-S129.

Balboni G, Salvadori S, Trapella C, Knapp BI, Bidlack JM, Lazarus LH, et al. (2010). Evolution of the Bifunctional Lead μ Agonist / δ Antagonist Containing the Dmt-Tic Opioid Pharmacophore. ACS Chem Neurosci 1(2): 155-164.

Bars Le, D, Gozariu M, Cadden SW (2001). Animal models of nociception. Pharmacol Rev. 53(4):597-652.

Bohn LM, Dykstra LA, Lefkowitz RJ, Caron MG, and Barak LS (2004). Relative opioid efficacy is determined by the complements of the G protein-coupled receptor desensitization machinery. Mol Pharmacol 66:106 –112.

Cahill CM, Morinville A, Lee MC, Vincent JP, Collier B, Beaudet A (2001). Prolonged morphine treatment targets delta opioid receptors to neuronal plasma membranes and enhances delta-mediated antinociception. Journal of Neuroscience. 21:7598–7607.

Chen TC, Cheng YY, Sun WZ, Shyu BC (2008). Differential regulation of morphine antinociceptive effects by endogenous enkephalinergic system in the forebrain of mice. Mol Pain 4:41.

Cheng Y, Prusoff WH (1973). Relationship between the inhibition constant (K1) and the concentration of inhibitor which causes 50 per cent inhibition (I50) of an enzymatic reaction. Biochem Pharmacol. 22: 3099–108.

Costantino CM, Gomes I, Stockton SD, Lim MP, Devi LA (2012). Opioid receptor heteromers in analgesia. Expert Rev Mol Med.14:e9.

Dang VC, Christie MJ (2012). Mechanisms of rapid opioid receptor desensitization, resensitization and tolerance in brain neurons. Br J Pharmacol. 165(6):1704-16.

Dietis N, Guerrini R, Calo G, Salvadori S, Rowbotham JD, Lambert GD (2009). Simultaneous targeting of multiple opioid receptors. A strategy to improve side effect profile. Br J Anaesth. 103 (1): 38-49

Dietis N, Rowbotham, JD, Lambert GD (2011). Opioid receptor subtypes: fact or fiction? Br. J. Anaesth. 107 (1): 8-18.

Dietis N, McDonald J, Molinari S, Calo G, Guerrini R, Rowbotham JD, Lambert GD (2012). Pharmacological characterisation of the bifunctional opioid ligand H-Dmt-Tic-Gly-NH-Bzl (UFP-505). *Br J Anaesth* 108(2): 262-70.

George SR, Fan T, Xie Z, Tse R, Tam V, Varghese G, O'Dowd BF (2000). Oligomerization of muand delta-opioid receptors. Generation of novel functional properties. J Biol Chem 275(34): 26128-35.

Gomes I, Jordan BA, Gupta A, Trapaidze N, Nagy V, Devi LA (2000). Heterodimerization of mu and delta opioid receptors: A role in opiate synergy. J Neurosci 20(22): RC110

Goodchild CS, Kolosov A, Geng L, Winter LL, Nadeson R (2009). Prevention and reversal of morphine tolerance by the analgesic neuroactive steroid alphadolone. Pain Med. 10(5):890-901.

Gupta A, Décaillot FM, Devi LA (2006). Targeting opioid receptor heterodimers: strategies for screening and drug development. AAPS J. 8(1):E153-9.

Harding SD, Sharman JL, Faccenda E, Southan C, Pawson AJ, Ireland S et al. (2018). The IUPHAR/BPS Guide to PHARMACOLOGY in 2018: updates and expansion to encompass the new guide to IMMUNOPHARMACOLOGY. Nucl Acids Res 46: D1091-D1106.

Hashimoto Y, Calo G, Guerrini R, Smith G, Lambert DG (2002). Effects of chronic nociceptin/orphanin FQ exposure on cAMP accumulation and receptor density in Chinese hamster ovary cells expressing human nociceptin/orphanin FQ receptors. Eur J Pharmacol. 449(1-2):17-22.

Hepburn MJ, Little PJ, Gingras J, Kuhn CM (1997). Differential effects of naltrindole on morphine-induced tolerance and physical dependence in rats. J Pharmacol Exp Ther 281(3): 1350-6

Huang P, Kehner GB, Cowan A, Liu-Chen LY (2001). Comparison of pharmacological activities of buprenorphine and norbuprenorphine: norbuprenorphine is a potent opioid agonist. J Pharmacol Exp Ther. 297(2): 688-95.

Kest B, Lee CE, McLemore GL, Inturrisi CE (1996). An antisense oligodeoxynucleotide to the delta opioid receptor (DOR-1) inhibits morphine tolerance and acute dependence in mice. Brain Res Bull. 39(3): 185-8

Keith DE, Murray SR, Zaki PA, Chu PC, Lissin DV, Kang L, Evans CJ, von Zastrow M (1996). Morphine activates opioid receptors without causing their rapid internalization. J Biol Chem. 271(32): 19021-4.

Khanna K and Pillarisetti S (2015). Buprenorphine – an attractive opioid with underutilized potential in treatment of chronic pain. J Pain Res. 8: 859–870.

Kilkenny C, Browne W, Cuthill IC, Emerson M, Altman DG (2010). NC3Rs Reporting Guidelines Working Group. Br J Pharmacol. 160:1577–1579.

Kitayama M, McDonald J, Barnes TA, Calo G, Guerrini R, Rowbotham DJ, Lambert DG (2007). In vitro pharmacological characterisation of a novel cyclic nociceptin/orphanin FQ analogue c[Cys(7,10)]N/OFQ(1-13)NH (2). Naunyn Schmiedebergs Arch Pharmacol. 375(6):369-76.

Koch T, Widera A, Bartzsch K, Schulz S, Brandenburg LO, Wundrack N, Beyer A, Grecksch G, Höllt V (2005). Receptor endocytosis counteracts the development of opioid tolerance. Mol Pharmacol. 67(1): 280-7.

Lambert DG (2008). The nociceptin/orphanin FQ receptor: a target with broad therapeutic potential. Nat Rev Drug Discov. (8):694-710.

Law PY, Erickson-Herbrandson LJ, Zha QQ, Solberg J, Chu J, Sarre A, Loh HH (2005). Heterodimerization of mu- and delta-opioid receptors occurs at the cell surface only and requires receptor-G protein interactions. J Biol Chem. 280(12):11152-64.

Leighton GE, Rodriguez RE, Hill RG, Hughes J (1988). k-opioid agonist produce antinociception after i.v. and i.c.v. but not intrathecal administration in the rat. Br J Pharmacol 93:553-560.

Louis F (2006). Transdermal buprenorphine in pain management – experiences from clinical practice: five case studies. Int J Clin Pract. 60(10): 1330–1334

Lutfy K and Cowan A (2004). Buprenorphine: A Unique Drug with Complex Pharmacology. Curr Neuropharmacol. 2(4): 395–402.

Madia PA, Dighe SV, Sirohi S, Walker EA, Yoburn BC (2009). Dosing protocol and analgesic efficacy determine opioid tolerance in the mouse. Psychopharmacology. 207(3):413-22.

McDonald J, Barnes TA, Okawa H, Williams J, Calo G, Rowbotham DJ, Lambert DG (2003). Partial agonist behaviour depends upon the level of nociceptin/orphanin FQ receptor expression: studies using the ecdysone-inducible mammalian expression system. Br J Pharmacol. 140(1): 61–70.

Micheli L, Di Cesare Mannelli L, Guerrini R, Trapella C, Zanardelli M, Ciccocioppo R, Rizzi A, Ghelardini C, Calo G (2015) Acute and subchronic antinociceptive effects of nociceptin/orphanin FQ receptor agonists infused by intrathecal route in rats. Eur J Pharmacol. 754:73-81

Morinville A, Cahill CM, Esdaile MJ, Aibak H, Collier B, Kieffer BL, Beaudet A (2003). Regulation of delta-opioid receptor trafficking via mu-opioid receptor stimulation: evidence from mu-opioid receptor knock-out mice. Journal of Neuroscience. 23:4888–4898.

Mosberg HI, Yeomans L, Anand JP, Porter V, Sobczyk-Kojiro K, Traynor JR, Jutkiewicz EM (2014). Development of a bioavailable μ opioid receptor (MOPr) agonist, δ opioid receptor (DOPr) antagonist peptide that evokes antinociception without development of acute tolerance. J Med Chem. 57(7): 3148-53

Nitsche JF, Schuller AG, King MA, Zengh M, Pasternak GW, Pintar JE (2002). Genetic dissociation of opiate tolerance and physical dependence in delta-opioid receptor-1 and preproenkephalin knock-out mice. J Neurosci 22(24): 10906-13

Paronis C and Bergman J (2011). Buprenorphine and Opioid Antagonism, Tolerance, and Naltrexone-Precipitated Withdrawal. J Pharmacol Exp Ther. 336(2): 488–495.

Pawar M, Kumar P, Sunkaraneni S, Sirohi S, Walker EA, Yoburn BC (2007). Opioid agonist efficacy predicts the magnitude of tolerance and the regulation of mu-opioid receptors and dynamin-2. Eur J Pharmacol. 563(1-3):92-101.

Schiller PW (2010). Bi- or multifunctional opioid peptide drugs. Life Sci. 86(15-16):598-603.

Sehgal N, Colson J, Smith HS (2013). Chronic pain treatment with opioid analgesics: benefits versus harms of long-term therapy. Expert Rev Neurother. 13(11):1201-20.

Stockton SD and Devi LA (2012). Functional relevance of μ-δ opioid receptor heteromerization: a role in novel signaling and implications for the treatment of addiction

disorders: from a symposium on new concepts in mu-opioid pharmacology. Drug Alcohol Depend. 121(3):167-72.

Storkson RV, Kjorsvik A, Tjolsen A, Hole K (1996). Lumbar catheterization of the spinal subarachnoid space in the rat. J Neurosci Methods 65:167–172.

Lawrence Toll, Girolamo Caló, Brian M. Cox, Charles Chavkin, MacDonald J. Christie, Olivier Civelli, Mark Connor, Lakshmi A. Devi, Christopher Evans, Graeme Henderson, Volker Höllt, Brigitte Kieffer, Ian Kitchen, Mary-Jeanne Kreek, Lee-Yuan Liu-Chen, Jean-Claude Meunier, Philip S. Portoghese, Toni S. Shippenberg, Eric J. Simon, John R. Traynor, Hiroshi Ueda, Yung H. Wong. Opioid receptors. Accessed on 07/03/2018. IUPHAR/BPS Guide to PHARMACOLOGY, http://www.guidetopharmacology.org/GRAC/FamilyDisplayForward?familyId=50.

Van Koppen CJ, Jakobs KH (2004) Arrestin-independent internalization of G protein-coupled receptors. Mol Pharmacol. 66(3):365-7.

Waldhoer M, Fong J, Jones RM, Lunzer MM, Sharma SK, Kostenis E, Portoghese PS, Whistler JL (2005). A heterodimer-selective agonist shows in vivo relevance of G protein-coupled receptor dimers. Proc Natl Acad Sci USA. 102(25):9050-5.

Wang J, Xu W, Zhong T, Song Z, Zou Y, Ding Z, Guo Q, Dong X, Zou W (2016). miR-365 targets β-arrestin 2 to reverse morphine tolerance in rats. Sci Rep. 6: 38285

Whistler JL and von Zastrow M (1998). Morphine-activated opioid receptors elude desensitization by -arrestin. Proc Natl Acad Sci USA 95:9914 –9919.

Whistler JL, Chuang HH, Chu P, Jan LY, von Zastrow (1999). Functional dissociation of mu opioid receptor signaling and endocytosis: implications for the biology of opiate tolerance and addiction. Neuron. 23(4):737-46.JI

Williams J, Ingram S, Henderson G, Chavkin C, Von Zastrow M, Schulz S, Koch T, Evans C Christie M (2013) Regulation of μ-Opioid Receptors: Desensitization, Phosphorylation, Internalization, and Tolerance. Pharmacol Rev. 65(1): 223–254.

Yaksh TL and Rudy TA (1976) Chronic catheterization of the spinal subarachnoid space. Physiology & Behavior. 17: 1013-1016.

Yang CH, Huang HW, Chen KH, Chen YS, Sheen-Chen SM, Lin CR (2011). Antinociceptive potentiation and attenuation of tolerance by intrathecal -arrestin 2 small interfering RNA in rats. Brit J. Anaesth. 107(5): 774-81

Yekkirala AS, Kalyuzhny AE, Portoghese PS (2010). Standard opioid agonists activate heteromeric opioid receptors: evidence for morphine and [d-Ala(2)-MePhe(4)-Glyol(5)]enkephalin as selective μ-d agonists. ACS Chem Neurosci. 1(2):146-54.

Yekkirala AS, Banks ML, Lunzer MM, Negus SS, Rice KC, Portoghese PS (2012). Clinically employed opioid analgesics produce antinociception via μ-δ opioid receptor heteromers in Rhesus monkeys. ACS Chem Neurosci. 3(9):720-7.

Zhang J, Ferguson SS, Barak LS, Bodduluri SR, Laporte SA, Law PY, and Caron MG (1998). Role for G protein-coupled receptor kinase in agonist-specific regulation of mu-opioid receptor responsiveness. Proc Natl Acad Sci USA 95:7157–7162.

Zhu Y, King MA, Schuller AG, Nitsche JF, Reidl M, Elde RP, Unterwald E, Pasternak GW, Pintar JE (1999). Retention of supraspinal delta-like analgesia and loss of morphine tolerance in delta opioid receptor knockout mice. Neuron 24(1): 243-52

Zuo Z (2005). The role of opioid receptor internalization and beta-arrestins in the development of opioid tolerance. Anesth Analg. 101(3):728-34, table of contents.

Dietis et al, Figure 1.
Functional assays (GTPγ^{35}S and cAMP) in CHO cells expressing MOP and DOP receptors

A

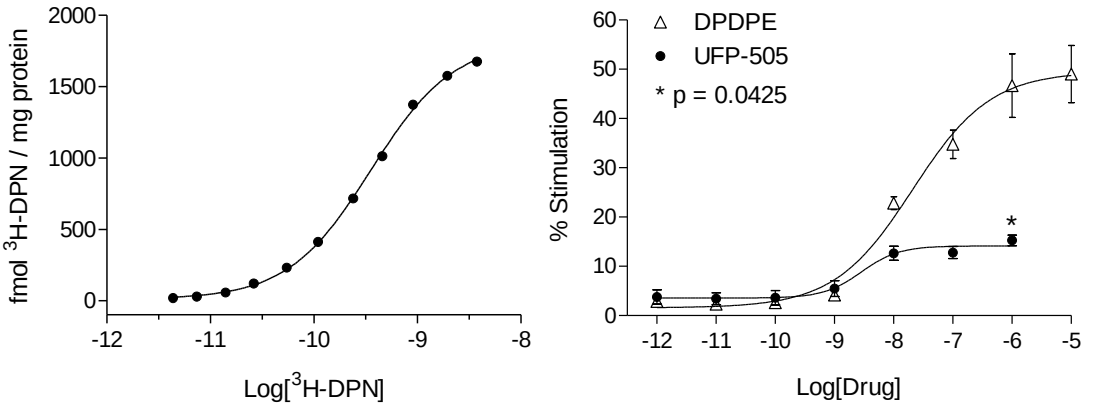

B

Cell-line	Forskolin	Forskolin + UFP-505	Forskolin + Reference ligand
CHO_{hMOP}	5.9 ± 2.9	1.9 ± 0.8 (82.6 %)	1.4 ± 1.0 (91.6 %) [Endomorphin-1]
CHO_{hDOP}	10.0 ± 0.4	8.3 ± 0.4 (18.3 %)	2.9 ± 0.1 (78.6 %) [DPDPE]

Figure 1. **In vitro pharmacological characterization of UFP-505 in CHO cells.**

[Panel A-left]: Representative curve of a single saturation experiment (from n=3 indicate density only) performed in CHO cells with high density of DOP receptors. *[Panel A-right]:* G-protein stimulation by UFP-505 and DPDPE ([D-Pen^{2,5}]-enkephalin) in these high expressing cells (n=5 per group). The maximum stimulation (E_{max}) achieved by UFP-505 binding (14.13%) was significantly higher (* $p<0.05$; t-test) than basal levels (unstimulated), whereas DPDPE produced an E_{max} of 49.55%.

[Panel B]: Effect of UFP-505 and reference agonists (DPDPE; 10 μM and Endomorphin-1; 1 μM) on forskolin-stimulated cAMP formation in CHO_{hMOP} and CHO_{hDOP} (lower expression) cells. All data are presented as mean ± SEM fold increase of basal stimulation (n=5-6). Percentage inhibition of cAMP is shown in parenthesis. Both DPDPE and Endomorphin-1 produced a significant inhibition compared to forskolin ($p<0.05$ by One-Way ANOVA with Bonferroni correction).

Dietis et al, Figure 2.

Opioid receptor internalization upon ligand binding

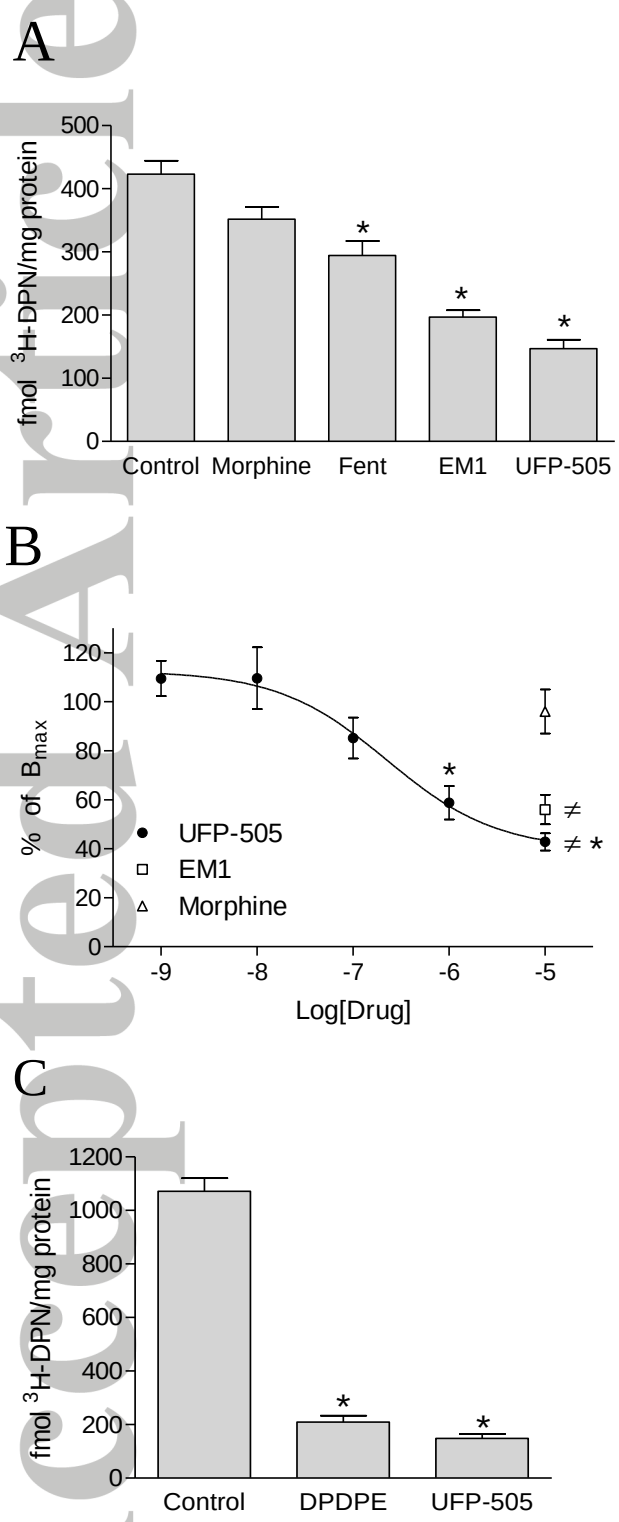

Figure 2. Opioid receptor internalization upon ligand binding.

[Panel A]: MOP receptor density (B_{max}; fmol ^{3}H-DPN/mg protein) in CHO_{hMOP} cells pretreated for 1h with various opioid ligands at 10 μM as determined from binding assays with saturating radioligand concentrations. Receptor internalization (†) is presented as a percentage of control.

The B_{max} values of all pre-treated cells except morphine were significantly different from control (*; $p<0.05$), as shown by One-Way ANOVA with Bonferroni correction test. *[Panel B]:* Effect of different concentrations of UFP-505 on MOP receptor internalization, compared with 10 μM endomorphin-1 and 10 μM morphine. UFP-505 internalizes the MOP receptor in a concentration-dependent manner. Data are normalized to a control (untreated) B_{max} (set to 100%). The pEC_{50} of the internalization curve was found to be 6.62 ± 0.17. An analysis of variance (One-Way ANOVA with Bonferroni correction test) revealed significant difference in the B_{max} at 1 μM and 10 μM UFP-505 when compared to that of control (*; $p<0.05$). Also, the 10 μM UFP-505 and EM1 treated cells showed significant difference in their B_{max} (≠; $p<0.05$) when compared with that of 10 μM morphine. *[Panel C]:* B_{max} of CHO_{hDOP} cells pre-treated with 10 μM UFP-505 or 10μM DPDPE for 1 hour. Receptor internalization (†) is presented as a percentage of control. The B_{max} values of pre-treated cells with UFP-505 and DPDPE were found to be significantly different compared to the control (*; $p<0.05$) by analysis of variance (One-Way ANOVA with Bonferroni correction test) and showed no significant difference between each other ($p>0.05$). All data are mean ± SEM from n=5-7.

Dietis et al, Figure 3.

Full saturation curves and loss of cell-surface receptors after treatment

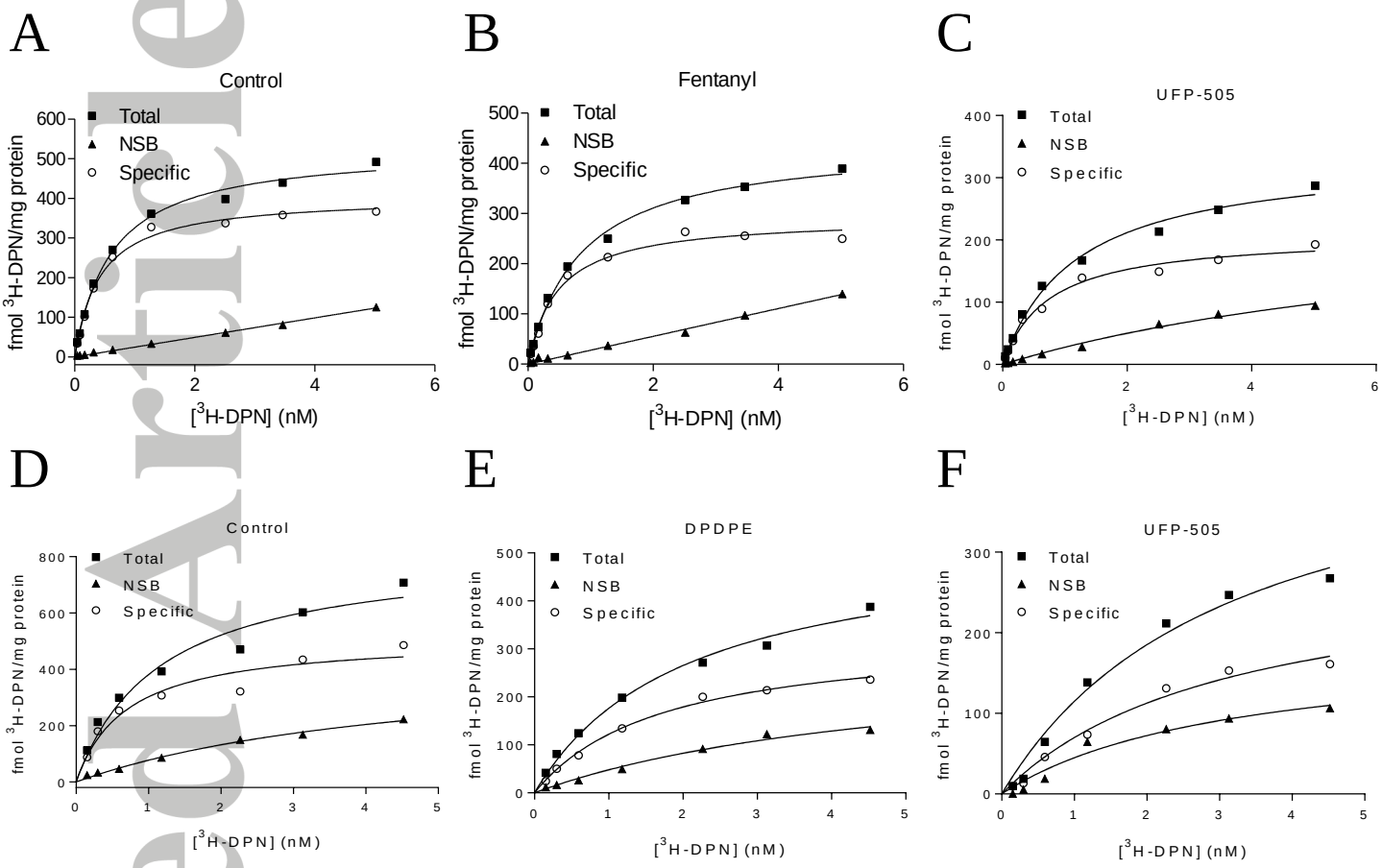

G

	CHO_{hMOP}			CHO_{hDOP}	
Treatment	***B_{max}***	***^{3}H-DPN pK_d***	***Treatment***	***B_{max}***	***^{3}H-DPN pK_d***
Control (untreated)	379 ± 63	9.14 ± 0.09	Control (untreated)	655 ± 82	9.05 ± 0.08
10μM fentanyl	247 ± 29 *	9.14 ± 0.10	10μM DPDPE	224 ± 39 *	8.90 ± 0.04
10μM UFP-505	120 ± 12 * #	9.03 ± 0.07	10μM UFP-505	105 ± 18 *	9.05 ± 0.03

Figure 3. Full saturation curves and loss of cell-surface receptors after treatment.

Internalization of opioid receptors is presented as a reduction in the B_{max} (fmol ^{3}H-DPN/mg protein) in full saturation binding curves of CHO_{hMOP} cells *(panel A, B and C)* and CHO_{hDOP} cells (*panel D, E and F*) pre-treated with 10 μM fentanyl, 10 μM DPDPE or 10 μM UFP-505 accordingly. The lack of effect on the radioligand K_d confirms that the reduced B_{max} reflects genuine receptor internalization. Representative hyperbola and sigmoidal saturation curves shown for MOP or DOP receptors from n=5 experiments. Collective B_{max} and pK_d values are presented as mean ± SEM in panel G. The B_{max} value of drug-treated cells was significantly lower (*$p<0.05$) compared to their respective untreated control (One-Way ANOVA with Bonferroni correction test), whereas the B_{max} of the UFP-505 treated cells was shown to be significantly lower to that of the fentanyl treated cells (# $p<0.05$). The same analysis has shown no significant differences in the pK_d between all groups.

Dietis et al, Figure 4.
Functional assay of β-arrestin recruitment after opioid treatment

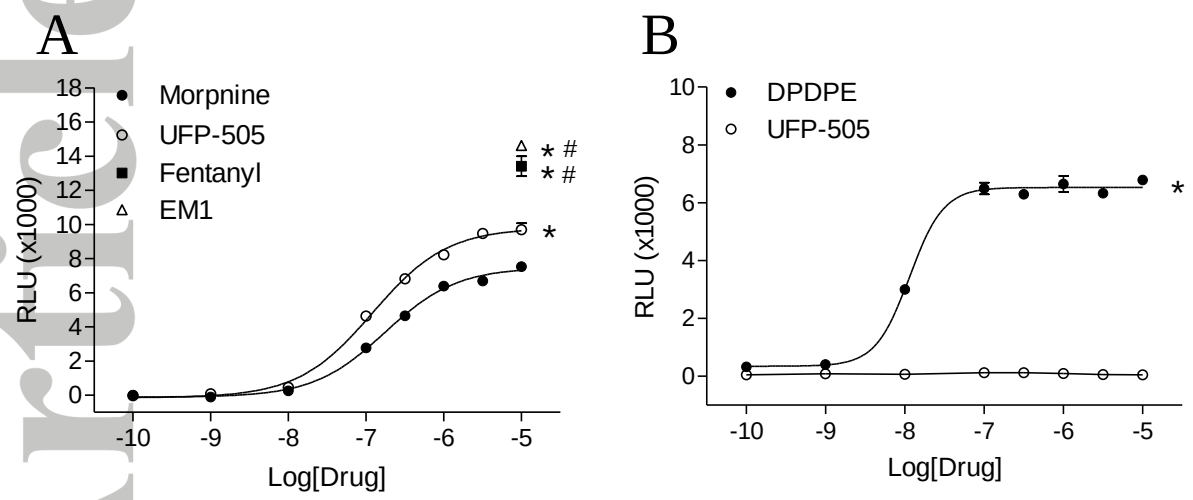

	Ligand	pEC_{50}	E_{max}
CHO_{hMOP} (Panel A)	Morphine	6.75 ± 0.07	7.51 ± 0.27
	UFP-505	6.91 ± 0.05	9.86 ± 0.33 *
	Fentanyl		13.40 ± 0.59 * #
	EM1		14.62 ± 0.25 * #
CHO_{hDOP} (Panel B)	DPDPE	7.93 ± 0.02	6.55 ± 0.16 *
	UFP-505	-	0.05 ± 0.01

Figure 4. Concentration-response curves for β-arrestin recruitment in CHO_{hMOP} and CHO_{hDOP} cells for various agents.

[Panel A]: morphine, fentanyl, EM1 and UFP-505 in CHO_{hMOP}. *[Panel B]:* DPDPE and UFP-505 in CHO_{hDOP}. Response is presented as relative luminescence units (RLU). Data are mean ± SEM of n=5 performed in duplicate. In the CHO_{hMOP} cells, no significant difference was found between the EC_{50} values produced from the morphine and UFP-505 curves ($p>0.05$ t-test). Comparing the 10 μM values among the different agents, the EM1, fentanyl and UFP-505 responses were all found to be significantly higher than that of morphine (*), whereas the EM1 and fentanyl responses were significantly higher than that of UFP-505 (#); there was no significant difference between the EM1 and fentanyl responses (analyzed by One-Way ANOVA with Bonferroni correction test; significance $p<0.05$). In the CHO_{hDOP} cells the E_{max} values of DPDPE was significantly higher than that of UFP-505 (Panel B; $p<0.05$ t-test).

Dietis et al, Figure 5.
In vitro characterization of a $CHO_{hMOP/hDOP}$ double-expression system

A

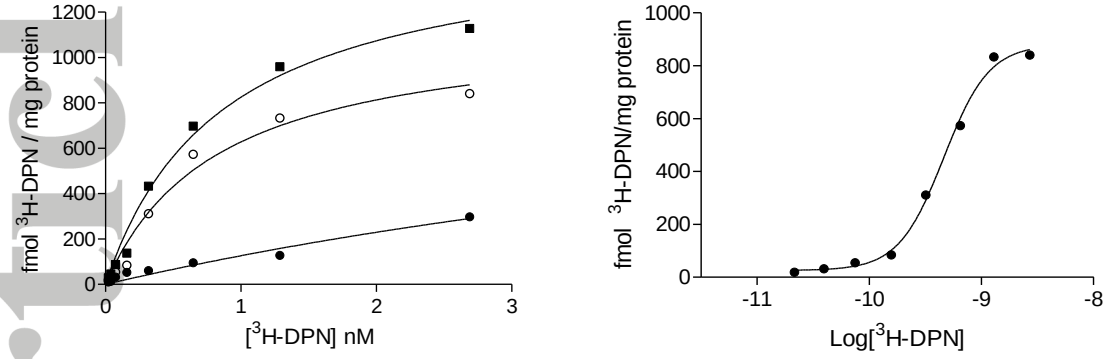

B

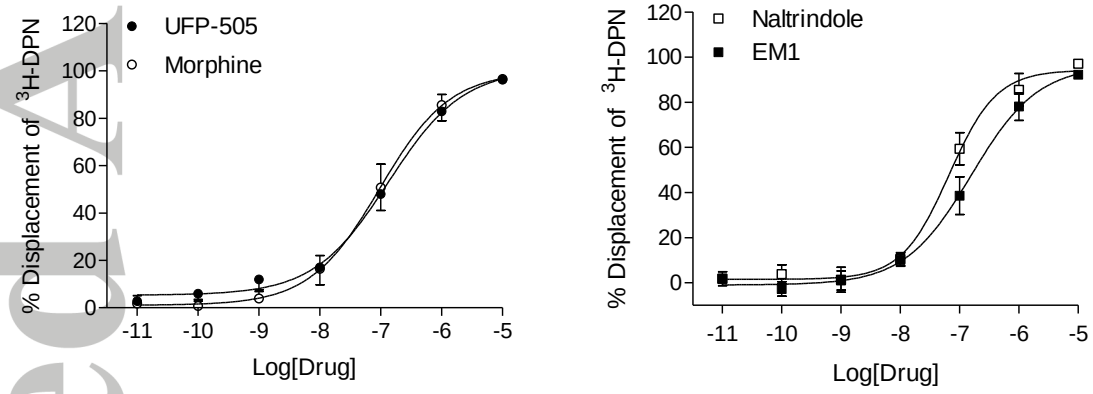

C

***CHO$_{hMOP/hDOP}$* pretreatment 1h**	**B_{max}**	**Internalizaton**
Control (CNT)	851±46	-
10μM Morphine (M)	812±59	4.48 %
10μM DPDPE	627±54	26.62 %
10μM EM1	482±60	43.33 %
10μM UFP-505	323±37	61.92 %

Figure 5. In vitro characterization of a $CHO_{hMOP/hDOP}$ double-expression system.
[Panel A]: Representative saturation binding curves (hyperbola; left and sigmoidal; right) performed on $CHO_{hMOP/hDOP}$ cell membranes with increasing concentrations of tritiated diprenorphine (^{3}H-DPN). Non-specific binding (NSB) was measured in the presence of 10μM Naloxone. Single representative curves are presented here from total n=3 (to indicate density only). The radioligand binding affinity was 9.51 (pK_d; K_d 30.9 nM). *[Panel B]:* Displacement of ^{3}H-DPN by UFP-505 and reference ligands (naltrindole, morphine and endomorphin-1; EM1) at $CHO_{hMOP/hDOP}$ cell membranes. Data are presented as mean ± SEM for n=5. Receptor

binding affinities (pK_i) of ligands were calculated using the Cheng-Prusoff equation; 7.70 ± 0.16 (UFP-505), 7.75 ± 0.11 (morphine), 7.53 ± 0.10 (EM1) and 7.87 ± 0.07 (naltrindole). *[Panel C]:* Receptor density (B_{max}, fmol ^{3}H-DPN/mg protein) and percentage internalization of receptors in $CHO_{hMOP/hDOP}$ cells pretreated for 1 hour with various ligands, using a saturating concentration of ^{3}H-DPN. Data are presented as mean±SEM values from n=3. Receptor internalization is presented as a percentage of control.

Dietis et al, Figure 6.
Receptor desensitization in $CHO_{hMOP/hDOP}$ cells.

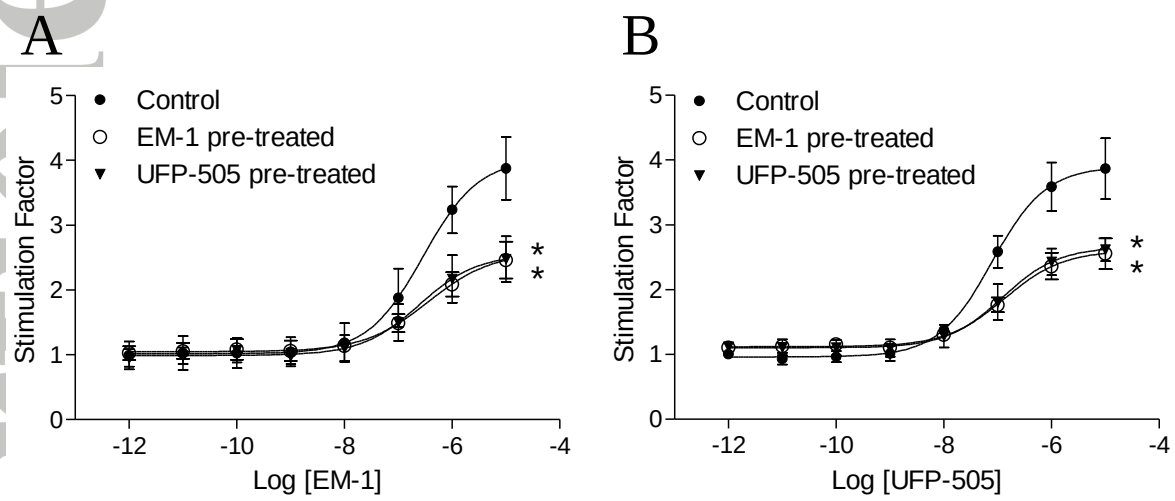

Pre-treatment 1h	Ligand challenge			
	EM-1 (Panel A)		UFP-505 (Panel B)	
	pEC_{50}	E_{max}	pEC_{50}	E_{max}
Control	6.55 ± 0.13	4.02 ± 0.23	7.10 ± 0.07	3.90 ± 0.46
10μM EM-1	6.49 ± 0.14	2.56 ± 0.13 *	6.90 ± 0.17	2.60 ± 0.23 *
10μM UFP-505	6.63 ± 0.17	2.55 ± 0.19 *	6.93 ± 0.15	2.65 ± 0.09 *

Figure 6. Receptor desensitization in $CHO_{hMOP/hDOP}$ cells.

Ligand-mediated GTPγ^{35}S binding measured in membranes prepared from $CHO_{hMOP/hDOP}$ cells after pre-treatment of $CHO_{hMOP/hDOP}$ cells with 10 μM EM-1 or 10 μM UFP-505 (control; no pre-treatment) for 1 hour and following a challenge with a range of concentrations of *[Panel A]* EM-1 or *[Panel B]* UFP-505. Data are expressed as mean ± SEM of n=5. There were no significant differences in the pEC_{50} of either EM-1 or UFP-505 comparing the pre-treatment values with the respective control. Pre-treatment E_{max} values were significantly lower than those of the control ($p<0.05$) for both EM-1 and UFP-505.

Dietis et al, Figure 7
Tail-flick test after acute intrathecal administration of UFP-505 in rats

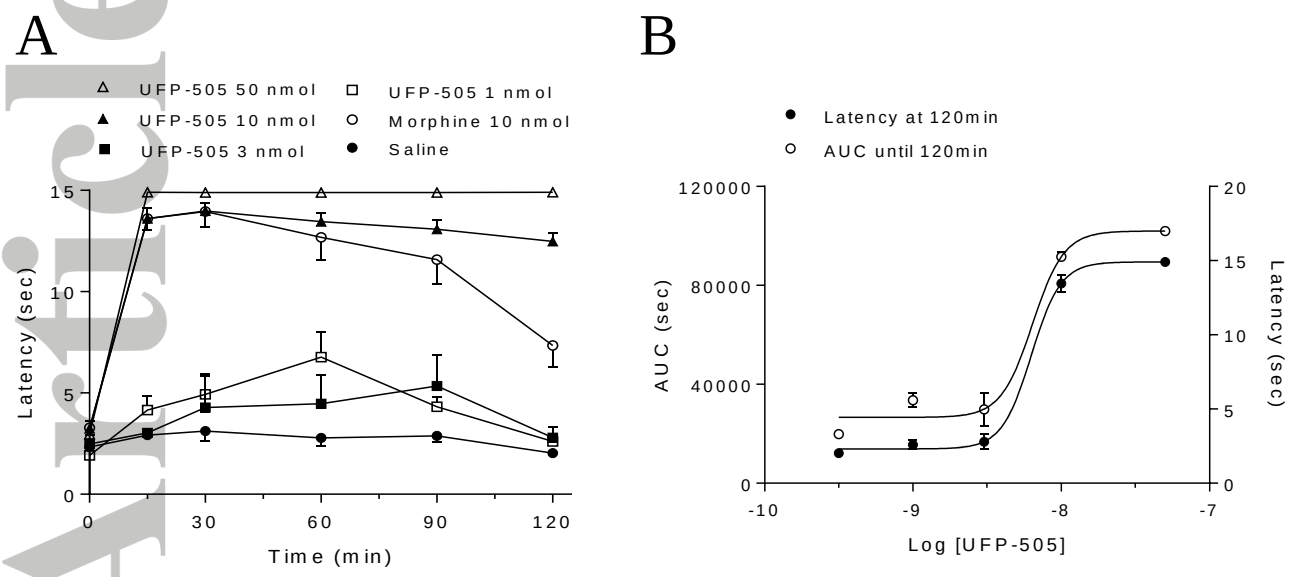

Figure 7. Acute intrathecal administration of UFP-505 in Tail Flick.

[Panel A]: Antinociceptive profile of acute intrathecal administration of saline (closed circles), UFP-505 (1 nmol; closed squares n=4, 3 nmol; open squares n=7, 10 nmol; closed triangles n=7, 50 nmol open triangles n=4) and morphine 10 nmol (open circles n=7) in rats using a tail-flick assay (15 sec cut-off time). Measurements were taken from 15 min to 120 min after a single drug administration. All groups had originally n=8 but due to a technical failure in catheter stabilisation (described in Methods), only the animals described by the n numbers here successfully completed the experiments. The antinociception recorded at 120 min after administration for UFP-505 at 10 nmol (n=7) was significantly higher than that of morphine 10 nmol (n=7, *p<0.005) *[Panel B]:* Dose-response curves for UFP-505 produced from the curves in panel A, for latency after 120 min of drug administration (expressing antinociception after 2 hours; closed circles) and the area under the curve (AUC in sec/min, expressing total antinociception; open circles). The antinociceptive potency of UFP-505 as produced from the 120 min latency curve was found 8.20 ± 0.05 (pEC_{50}; EC_{50} 6.27 nmol), whereas the potency from the AUC curve was found 8.19 ± 0.18 (pEC_{50}; EC_{50} 6.38 nmol). Data presented as mean ± SEM.

Dietis et al, Figure 8.
Paw-pressure test after continuous intrathecal administration of UFP-505 in rats

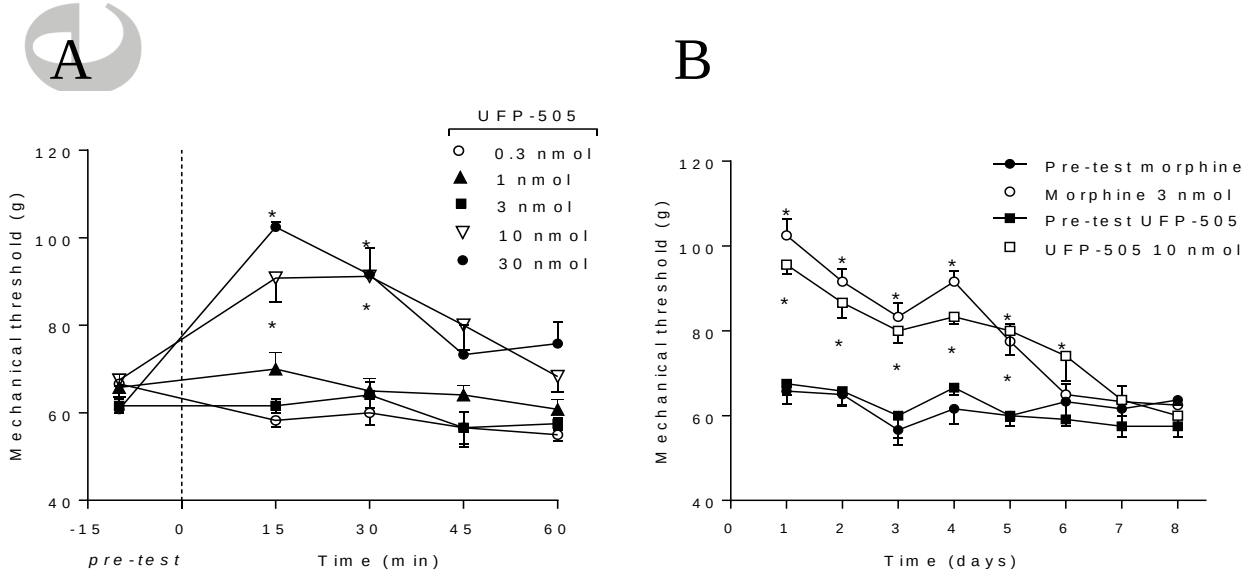

Figure 8. **Intrathecal administration of UFP-505 in Paw Pressure.**

[Panel A]: Antinociceptive effect of acute intrathecal administration of UFP-505 in paw pressure test. The compound was dissolved in saline solution and a final volume of 10 µl was administered at the lumbar level of the spinal cord by intrathecal catheter. Antinociception was evaluated by Paw pressure test. 30 nmol UFP-505 impaired locomotor activity of the posterior paws (see table 1, * $p<0.05$ compared to pre-test values). *[Panel B]:* Antinociceptive effect of repeated intrathecal administration of UFP-505 and morphine in a paw-pressure test. The compounds were dissolved in saline solution and a final volume of 10 µl was administered at the lumbar level of the spinal cord by intrathecal catheter. The treatment was daily repeated and antinociception was evaluated 30 minutes after administration by Paw pressure test (* $p<0.05$ compared to their corresponded pre-test values). All data are mean ± SEM, n=8.

Dietis et al, Table 1.
Effect on motor coordination evoked by acute spinal administration of UFP-505.

Compound (nmol/intrathecal)	Motor coordination (number of falls)				
	Pretest	After treatment (minutes)			
		15'	*30'*	*45'*	*60'*
UFP-505 0.3	0	0	0	0	0
UFP-505 1	0	0	0	0	0
UFP-505 3	0	0	0	0	0
UFP-505 10	1.0 ± 0.5	1.0 ± 0.5	0	0	0
UFP-505 30	0	6 ± 0	nd	nd	Nd

Table 1. Effect on motor coordination evoked by acute spinal administration of UFP-505. The compound was dissolved in saline solution and a final volume of 10 µl was administered at the lumbar level of the spinal cord by intrathecal catheter. Motor coordination was evaluated by rotarod test measuring the number of falls in 60 seconds. The 30 nmol UFP-505 dose impaired locomotor activity of the posterior paws. All data are mean ± SEM, n=8.

Dietis et al, Table 2.
Opioid receptor density in tissues from acute intrathecally-treated rats

Tissue	Treatment	MOP		DOP	
		B_{max}	*Intern.*[†]	B_{max}	*Intern.*[†]
Frontal cortex	*Saline*	73.85 ± 5.50		91.68 ± 8.71	
	Morphine	71.64 ± 3.51	3 %	96.77 ± 3.09	-5.5 %
	UFP-505	46.91 ± 1.66	36.5 %	40.24 ± 1.31	56.1 %
Spinal cord	*Saline*	23.08 ± 1.94		33.12 ± 3.21	
	Morphine	21.44 ± 0.99	7.1 %	32.54 ± 3.85	1.8 %
	UFP-505	12.76 ± 2.40	44.7 %	18.86 ± 2.08	43.1 %

Table 2. In vitro analysis of neuronal tissue taken from intrathecally-treated rats.

Receptor density (B_{max}; fmol radioligand / mg protein) of MOP and DOP receptors as produced from binding experiments with saturating concentration of radioligand in extensively washed membranes prepared from the frontal cortex and spinal cord tissue, taken from rats treated acutely with either 10 nmol UFP-505 or 10nmol morphine. Saturation assays were performed using ^{3}H-DAMGO (≈ 6.7 nM) and ^{3}H-NT (≈ 3.3 nM) respectively. Only the UFP-505 treated animals showed a reduction in both MOP and DOP B_{max}, in both tissues. Data are expressed as means ± SEM for n=3-4.